Study on the Optimal Access Orbiter Selection Algorithm in Mars Automatic Relay Communications

PENG WAN, Student Member, IEEE
YAFENG ZHAN
XIAOHAN PAN
Tsinghua University, Beijing, China

In current Mars relay communications, the Consultative Committee for Space Data Systems (CCSDS) Proximity-1 protocol is simple and efficient but it exhibits low flexibility in optimal access orbiter selection. Once connected with the first successful hailing orbiter, the rover would not switch to other better orbiters until the end of that connection, which makes it difficult to provide more convenient and efficient data relay services. The entire system cost is essential for optimal access orbiter selection, which includes both the Proximity-1 links' transmission cost concerned with the data transmission energy consumption and the orbiters' storage cost concerned with the data buffering energy consumption, thus minimizing the system cost on unit data volume could reduce energy consumption and extend the deep space vehicle's life. We employ long-term simulations of the single rover, simultaneously tracking two orbiters utilizing the improved Hotelling oligopoly model, and reveal the potential improvements for the current "first-come first-serve" selection strategy. In this article, a complete solution is proposed to solve the optimal access orbiter selection issues, including the geometric model, orbit design, oligopoly model, storage cost, and optimal selection algorithms. Simulation results show that our new algorithm outperforms current CCSDS Proximity-1 protocols and distance-dependent selection algorithm in the system cost on unit data volume with the selection gains 36.14% and 29.59%, respectively, which could be used as the rover's optimal access orbiter selection algorithm in Mars automatic relay communications.

Manuscript received July 15, 2019; revised October 31, 2019; released for publication November 20, 2019. Date of publication November 26, 2019; date of current version August 7, 2020.

DOI. No. 10.1109/TAES.2019.2955811

Refereeing of this contribution was handled by M. De Sanctis.

This work was supported in part by the National Natural Science Foundation of China under Grant 61671263 and Grant 61971261 and in part by theTsinghua University Independent Scientific Research Project under Grant 20194180037.

Authors' address: P. Wan, Y. Zhan, and X. Pan are with the Space Center and the Beijing National Research Center for Information Science and Technology, Tsinghua University, Beijing 100084, China, E-mail: (wanp16@mails.tsinghua.edu.cn; zhanyf@tsinghua.edu.cn; pxh15@mails.tsinghua.edu.cn). *(Corresponding author: Yafeng Zhan.)*

I. INTRODUCTION

During the Mars rover exploration phase, it is necessary to send the Mars surface exploration data back to Earth for scientific research and other important applications. In order to enhance the data transmission capacity, the Earth station is designed to be powerful enough with an antenna of about 70 m diameter; however, due to the large deep space distance between the Earth and Mars [1], along with the planet rotation and revolution, the backward data transmission rate is still as low as several bits per second—being constrained by the simple direct-to-Earth (DTE) link transmitters on the Mars rover.

In order to further improve the data transmission capacity, several data relay proposals have been studied and developed in past years, such as the Lagrange points L4/L5 of the Sun–Earth system [2], the solar system satellite relay constellation [3], and the Mars orbiter relay communication [4]–[6]. In the current space mission, the Mars orbiter relay communication proposal is widely used in most of the international Mars surface exploration missions by NASA and ESA [7], such as NASA Mars Odyssey, ESA Mars Express, etc.

The near-Mars link between the rovers and orbiters is usually called the "proximity link," as shown in Fig. 1, which is characterized by the dynamically changing distance and complicated medium access control procedures. The Consultative Committee for Space Data Systems (CCSDS) has studied and recommended a series of "Proximity-1" protocols with the orbiter-mastered hailing channel and single-access working channel related to the Mars relay communications [8]. CCSDS Proximity-1 protocols are assembled in software-defined equipment on most of the Mars orbiters [9], [10] and rovers [11], along with the adaptive coding and modulation (ACM) mechanism, which have obviously increased the backward data volume as compared with the DTE link in the past Mars exploration missions.

When there are multiple orbiters and rovers, the key point of such access technology could be summarized as "single access, random back-off, first-in first-serve," with the procedure shown in Fig. 2, which aims to simplify the complexity of the rover communication equipment. However, there will likely be more and more rovers and orbiters in the future according to the plans for Mars exploration and immigration, and the CCSDS Proximity-1 protocols might not be able to provide automatic and efficient access control mechanisms. The main challenges are listed as follows.

1) Lack of fairness: When two Rovers R_1 and R_2 are covered by one Orbiter S_1, only one Rover R_1 can get access to the Orbiter S_1. The multiple users' access problem has been studied in [12].
2) Lack of choice: When one Rover R_M is covered by two Orbiters S_2 and S_N, only one Orbiter S_2 can be chosen as the access point. The access interact

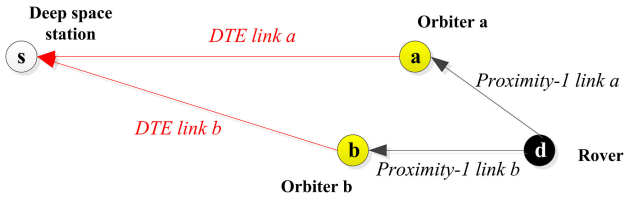

Fig. 1. Mars orbiter relay communication diagram.

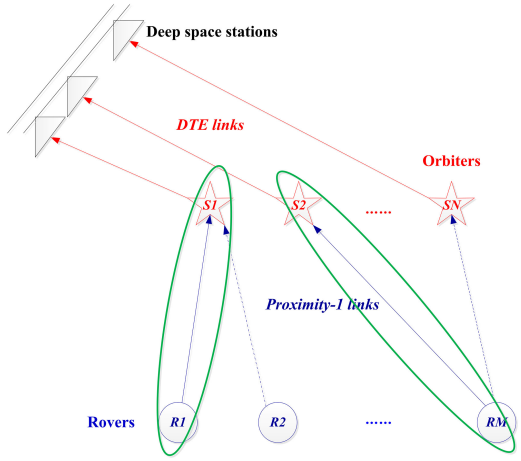

Fig. 2. Characteristics of current multiple orbiters and rovers relay communication.

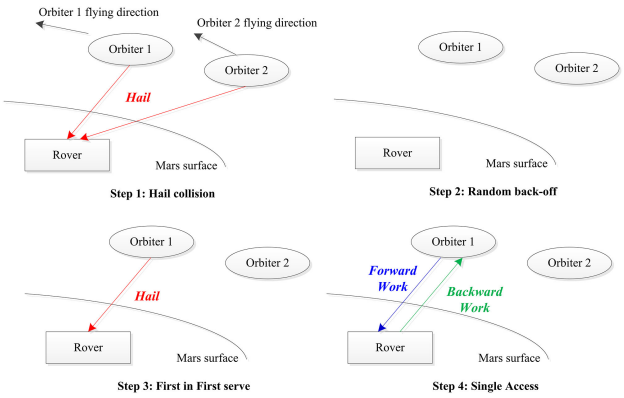

Fig. 3. CCSDS Proximity-1 multiple orbiters and single rover access interact procedure.

procedure can be seen in Fig. 3. The optimal selection problem will be studied in this article.

In current Earth satellite communications, the most studied access selection schemes [13] include the following.

1) Distance dependence: The ground station selects the access satellite by space distance, which is widely used in satellite constellation circumstance.
2) Time dependence: The ground station selects the access satellite by contact time.
3) Hybrid scheme: The ground station selects the access satellite by both distance and contact time.

However, there are some shortcomings associated with these selection schemes. First, the current methods perform well on the user access to low-Earth satellite constellations

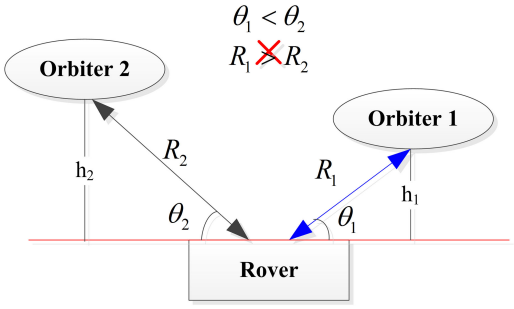

Fig. 4. Distances between single rover and multiple orbiters with different elevation angles.

under the situation that all the satellites are located on the isomorphic orbits, because the space distance and contact time period are both determined by the elevation angle, which means that the smaller elevation angle corresponds to larger space distance and longer contact time. For Mars relay communications, the orbiters usually locate on heterogeneous orbits for different exploration purposes, so that the orbiter with smaller elevation angle might not be of the larger space distance, as shown in Fig. 4. Second, the current methods mainly concern with the data transfer capability, without consideration on the availability of orbiter's storage space. In addition to Mars relay communications, the Mars orbiters also undertake other important exploration missions, which require the resource sharing of limited storage space. Therefore, current access selection schemes should be further improved based on the characteristics of Mars relay communications.

II. SYSTEM MODEL

A. Terms and Definitions

1) Coordinate system: Two-dimensional (2-D) cartesian coordinate system, marked as x-o-y.
2) Small circle: The orbiter coverage edge with lower altitude h_1 and radius D_1 marked as Orbiter 1.
3) Large circle: The orbiter coverage edge with higher altitude h_2 and radius D_2 marked as Orbiter 2.
4) Line-of-circles: The horizontal line from small circle center to large circle center, marked as D_{12}.
5) Edge point: The intersection of the circle and the line-of-circles, marked as E_{p1} on small circle and E_{p2} on large circle.
6) Edge forwarding terms: The distance between two edge points, marked as $d_{Ep12} = E_{p1} - E_{p2}$.
7) Cross coverage area: The intersection area of the small and large circles, marked as A.
8) Right cross subarea: The subarea of the cross coverage area in the right side of the vertical line through the rover, marked as S_{right}.
9) Relative geometry weight: The probability of different relationships between two orbiters based on the 2-D relative geometric positions, marked as w.

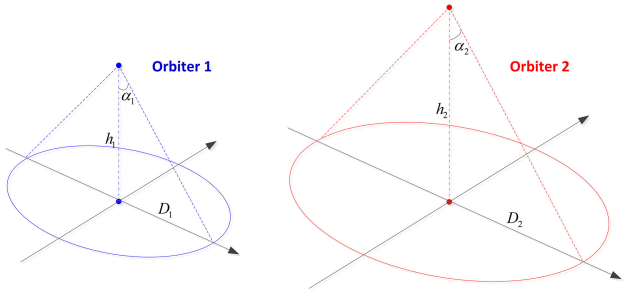

Fig. 5. Independent coverage of Orbiters 1 and 2 with different altitudes.

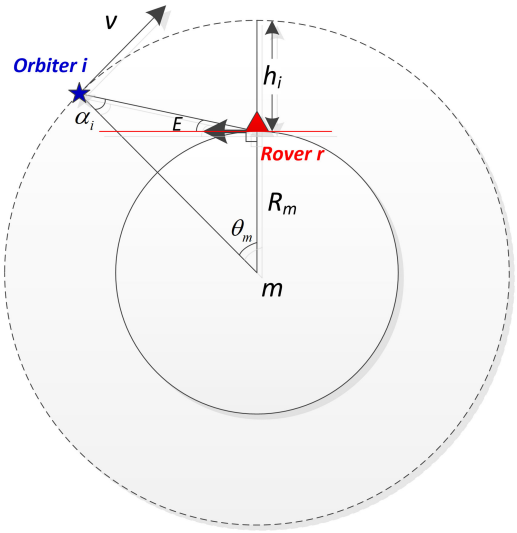

Fig. 6. Observation geometry between rover and obiters concerned with elevation angle.

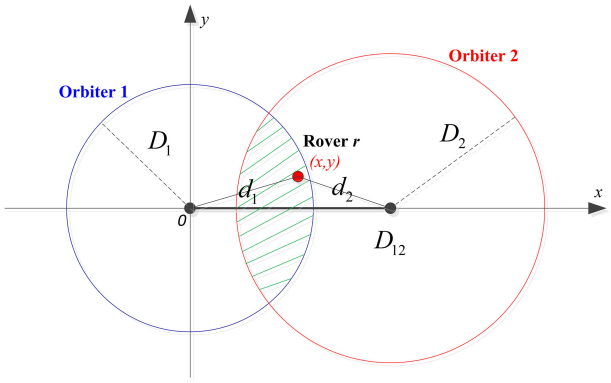

Fig. 7. Cross coverage area of Orbiters 1 and 2 (shown as green shadow).

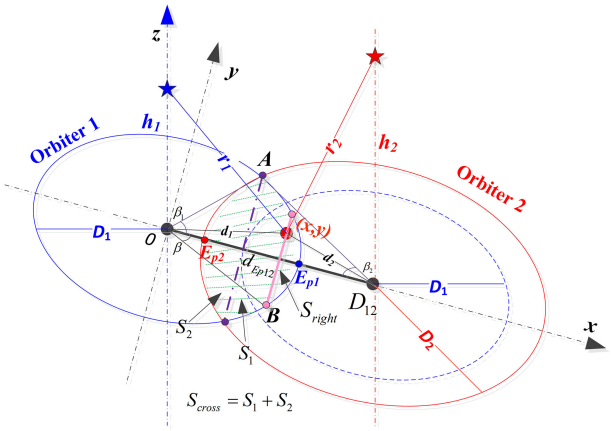

Fig. 8. Geometric model for cross coverage area.

B. Geometric Model

Fig. 5 describes the 3-D geometric model of the different altitude orbiters' beam coverage, where the parameter $\alpha_i (i = 1, 2)$ means the antenna's half beam width, h_i means the orbiter's average altitude above the Mars surface, and D_i means the orbiter's coverage radius on the Mars surface, which could be calculated by the equation $D_i = h_i \times \tan(\alpha_i)$. Without loss of generality, the altitude of Orbiter 1 is lower than Orbiter 2 ($h_1 < h_2$). In order to provide better data relay communication, the orbiter's antenna is usually omnidirectional, and α_i could be calculated by (1), as shown in Fig. 6

$$\frac{\sin(90^\circ + E)}{R_m + h_i} = \frac{\sin(\alpha_i)}{R_m} \tag{1}$$

where E is the observation elevation angle of Rover r (usually 5° in regular space engineering), v is the velocity vector of Orbiter i, h_i is the Orbiter i's altitude, and R_m is the Mars mean radius.

Fig. 7 describes the 2-D geometric model of Orbiters 1 and 2 covering Rover r in the x-o-y coordinate system, where the subastral point of Orbiter 1 is located at the original point $(0, 0)$, the subastral point of Orbiter 2 is located at the x-axis with the coordinate $(D_{12}, 0)$, D_{12} is the distance between the two orbiters' subastral point, Rover r is located at the point (x, y), d_1 is the distance between Rover r and the subastral point of Orbiter 1, and d_2 is the distance between Rover r and the subastral point of Orbiter 2. The distance between Rover r and two orbiters are $r_1 = \sqrt{d_1^2 + h_1^2}$ and $r_2 = \sqrt{d_2^2 + h_2^2}$, respectively, where $d_1 = \sqrt{x^2 + y^2}$, $d_2 = \sqrt{(D_{12} - x)^2 + y^2}$.

Fig. 8 describes the 3-D geometric model, which is used to analyze the cross coverage area distribution issues, and the parameters are defined as follows.

1) x-y-z is the Cartesian coordinate of the 3-D geometric model, with Orbiter 1's subastral point located at the origin O and Orbiter 2's subastral point located at D_{12}, with $D_{12} = D_1 + D_2 - d_{Ep12}$.
2) h_i is the altitude of Orbiter i, $i = 1, 2$.
3) d_i is the surface distance between rover and the subastral point of Orbiter i.
4) r_i is the space distance between rover and Orbiter i.
5) A is the positive intersection of two circles, with $\overrightarrow{OA} = D_1$ and $\overrightarrow{D_{12}A} = D_2$.
6) B is the negative intersection of small circle and the vertical line through rover, with $\overrightarrow{OB} = D_1$.

7) β is the angle between the vector $\overrightarrow{OD_{12}}$ and $\overrightarrow{OB}$, as $\beta = \arccos(\frac{x}{D_1})$.

8) β_1 is the angle between the vector $\overrightarrow{OD_{12}}$ and $\overrightarrow{OA}$, as $\beta_1 = \arccos(\frac{D_1^2+D_{12}^2-D_2^2}{2D_1D_{12}})$.

9) β_2 is the angle between the vector $\overrightarrow{D_{12}O}$ and $\overrightarrow{D_{12}A}$, as $\beta_2 = \arccos(\frac{D_2^2+D_{12}^2-D_1^2}{2D_2D_{12}})$.

C. Constrains and Assumptions

1) *Contact Events:* The optimal orbiter selection issue should be constrained in such contact periods that the rover are simultaneously tracking two orbiters, which could be defined by $\{\bigcup_n \mathrm{CT}_{r1}^n\} \bigcap \{\bigcup_m \mathrm{CT}_{r2}^m\}$, where CT denotes the contact time period, superscript n, m denote the contact sequences, subscript r denotes the Mars rover, and subscript 1, 2 denote the Mars Orbiters 1 and 2.

2) *Data Rates:* ACM mechanism embedded in current Mars orbiters [9], [10] and rovers [11] ensures data rate changes adaptively with dynamic channel status, which means that with the decrease of space distance between the rover and orbiter, the data rate increases gradually according to CCSDS Proximity-1 protocols [14]–[16] as rate $= 2^n$[kb/s], $n = 0, 1, 2, \ldots, 12$, from 1 kb/s to 4096 kb/s.

3) *Data Volumes and Storage Space:* For Mars rover, it is assumed that the rover has a massive detection data source, which could send the backward data continuously in any contact event. For Mars orbiter, it is assumed that each orbiter has the limited data storage space of the same buffer size for data transmission, and the initial storage space status for Mars relay communications might be influenced by other exploration tasks and diverse in different contact events. In this article, the buffer size is defined as the upper bound of the data transmitted by any single orbiter independently in our simulation, and the initial storage space status is defined as the initial storage percentage, that is, the ratio of storage space used by other Mars exploration tasks to total available buffer size, which is the important initial condition in our simulation.

D. Optimization Function

1) *System Cost Function:* In this article, both the space distance and storage percentage are considered in the entire system cost, which includes the transmission cost concerned with the data transmission energy consumption and the storage cost concerned with the data buffering energy consumption, thus minimizing the system cost on unit data volume could reduce energy consumption and extend in deep space vehicle's life. The entire system cost function could be described as (2) by the weighted summation method, both the space distance r and storage percentage q should be considered in the optimal selection decisions, because the space distance is related to Proximity-1 link transmission capacity in each time slot based on current adaptive coding and modulation mechanism, and the storage percentage is related to the orbiters' data storage capability based on buffer shared with other scientific tasks

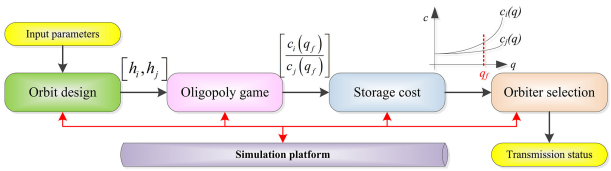

Fig. 9. Algorithm architecture for optimal orbiter selection.

$$C_\tau(q, r) = \lambda \cdot c(q) + t(r) = \lambda \cdot A \cdot \left(1 - q\right)^{-\alpha} + t \cdot r^2 \tag{2}$$

where $C_\tau(q, r)$ denotes the system cost function in the τth time slot, $c(q)$ denotes the storage cost function, $t(r)$ denotes the transmission cost function related to the distance between the rover and orbiters, q denotes the orbiters storage percentage, that is, the ratio of utilized storage space to total available buffer size for data transmission, α denotes the power factor for each storage curve function, r denotes the space distance, and A and t denote the magnitude balance factor between storage cost and transmission cost, calculated by the space distance as $1/\max(r^2)$ and storage percentage as $1/\max((1-q)^{-\alpha})$, respectively, λ is the parameter to adjust the weights of storage cost and transmission cost.

2) *Optimization Objective:* As we all known, the power supply subsystem is the essential component in deep space vehicle, and the vehicles effective life is related to the total power consumption. Zhu [17] evaluated the relationship between the battery capacity C_B and the depth of discharge (DOD) as $C_B = \frac{P_e \cdot T_e}{\mathrm{DOD} \cdot N_e \cdot \eta_e}$, where P_e is the power consumed during the shadow period T_e, N_e is the number of batteries, and η_e is the battery conversion efficiency. The equation shows that the battery's DOD is inverse proportional to its capacity C_B, which means that if the Mars relay communications consume more power, it is necessary to increase C_B, which leads to lower DOD. Based on the relationship between the DOD and space vehicle's effective life described in [17], the lower DOD responds to the later period in effective life. Consequently, the balance between the on-orbit energy consumption and the space vehicle's effective life should be reasonably considered in a comprehensive design.

Therefore, in this article, the optimization objective is the minimization of system cost on unit data volume as $\min\{\frac{\sum_\tau C_\tau(q,d)}{\sum_\tau \mathrm{TP}_\tau}\}$, where TP_τ denotes data transmission throughput in τth time slot. The optimization objective means that each orbiter should try best to transfer the data as much as possible, however, both the transmission cost on the Proximity-1 links and the storage cost on orbiters should also be considered in order to provide the better data relay services in a relatively longer time period.

III. OPTIMIZATION ALGORITHM

A. Algorithm Architecture

The solution architecture consists of several serial steps as shown in Fig. 9, in which the terms are defined as follows.

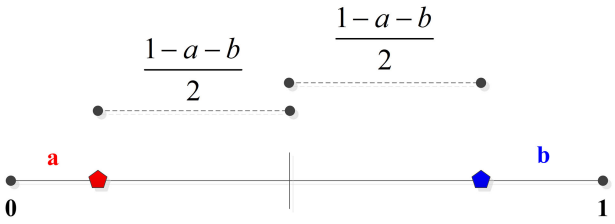

Fig. 10. Classical Hotelling model.

1) Input parameters are the repeated ground track parameters for each orbiter.
2) Orbit design is the repeating planet surface track orbit design according to the input parameters, with the outputs as the different orbiter altitudes $[h_i, h_j]$.
3) Oligopoly model is the improved oligopoly model with Nash equilibrium (NE) prices according to the orbiter altitudes, with the output as the price ratio $[c_i(q_f)/c_j(q_f)]$, where q_f is the storage threshold.
4) Storage cost is the storage cost prove and analysis according to the price ratio, with the outputs as the storage cost functions $[c_i(q), c_j(q)]$.
5) Orbiter selection is the optimal orbiter selection for the rover according to the storage cost functions and orbiter parameters, with the outputs as the transmission status in time sequences.
6) Transmission status is total data transmission volume, total cost, average cost in unit data volume, and the selected orbiter at each time slot.
7) Simulation platform is performance evaluation based on above models and relevant parameters.

B. Oligopoly Game

The optimal orbiter selection issue is equivalent to the price competition of several oligopolies in economics, in which the orbiters act as the oligarchs to supply data relay services and the rovers act as the customers to buy the services from different oligarchs. The NE price solution could be considered as the orbiter's current storage service price for unit data volume, and the ratio between any two orbiters could be used as the input parameter for the storage cost function.

1) *Classical Hotelling Model:* In order to explain the location selections and price decision actions in the Oligopoly market, the American economist H. Hotelling proposed the Hotelling model [18] in 1929. In this model, different suppliers provide identical services, but consumers located in different positions pay for different transport costs. Therefore, the consumers should focus on the balance between service prices and transport costs.

Fig. 10 shows the classical Hotelling model of two suppliers, with all the consumers and suppliers located at 1-D coordinate axis of unit length. Assuming that 1) suppliers 1 and 2 are located at a and $1-b$, respectively; 2) $1-a-b \geq 0$; and 3) transport cost is a quadratic function as $t \cdot d^2$, where t denotes the distance cost index and d denotes the distance between consumer and supplier, let x denote the consumer's location, $D_i (i = 1, 2)$ denote the consumer's purchase probability for supplier i, and p_i denote the price of supplier i. Then, we get the following.

1) Equilibrium equation: $p_1 + t \cdot (a-x)^2 = p_2 + t \cdot (1-b-x)^2$.
2) NE price: $p_1^*(a,b) = c + t \cdot (1-a-b) \cdot (1 + \frac{a-b}{3})$, $p_2^*(a,b) = c + t \cdot (1-a-b) \cdot (1 + \frac{b-a}{3})$.

TABLE I
Differences Between Hotelling Model and Orbiter Selection

Items	Hotelling model	Orbiter selection
Model dimension	The consumer and suppliers locate at 1-d coordinate axis of unit length.	The cross coverage area of two orbiters over single rover is a 2-d region on Mars surface.
Supplier limits	Each supplier locates at fixed location.	The orbiters locate at different orbits with dynamical cross coverage areas.
Consumer distribution	The consumer locates on the axis with uniform distribution probability.	The distribution probability changes dynamically over the relative geometric relationship between two orbiters.

2) *Similarities and Challenges:* From the description abovementioned, we could find that there are many mathematical similarities between the Hotelling model and orbiter selection issue.

1) Hotelling model introduces distance to evaluate the transport cost, which should also be considered in orbiter selection issue, because the transmission loss is mainly determined by the space distance between the rover and orbiters.
2) Equilibrium equation utilizes a quadratic function to define the transport cost, which coincides with the wireless channel propagation model.
3) NE price is symmetry in mathematical form, which could eliminate the directional differences for modeling simplicity when the orbiters fly over the rover from different directions.

Therefore, it is reasonable for us to utilize the Hotelling model as mathematical reference to design our oligopoly game optimization algorithm. However, there are still some differences between this model and the Mars automatic relay communications scenario, as shown in Table I.

3) *Improved Hotelling Model:* In order to build the available oligopoly game model for the Mars automatic relay communications, we revise the classical Hotelling model according to abovementioned challenges with following analysis.

a) Utilize cross coverage area S_{cross} to evaluate the double orbiters system relay capability: The cross coverage area S_{cross} is concerned with the geometric relationship between two orbiters, it is obviously that the larger S_{cross} is equivalent to higher rover access probability, that is, the double orbiters system could provide better data relay service capability. The cross coverage area S_{cross} shown as the green shadow in Fig. 8 is divided into two parts, respectively, marked as S_1 and S_2, where

$$\begin{aligned} S_1 &= \beta_1 \cdot D_1^2 - \sin\beta_1 \cdot \cos\beta_1 \cdot D_1^2 \\ &= \left(\beta_1 - \frac{1}{2}\sin 2\beta_1\right) \cdot D_1^2 \end{aligned} \tag{3}$$

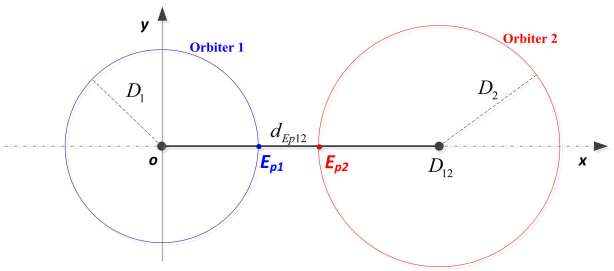

Fig. 11. Geometric model of stage 1.

$$S_2 = \beta_2 \cdot D_2^2 - \sin\beta_2 \cdot \cos\beta_2 \cdot D_2^2 = \left(\beta_2 - \frac{1}{2}\sin 2\beta_2\right) \cdot D_2^2 \tag{4}$$

$$S_{\text{cross}} = S_1 + S_2 = \left(\beta_1 - \frac{1}{2}\sin 2\beta_1\right) \cdot D_1^2 + \left(\beta_2 - \frac{1}{2}\sin 2\beta_2\right) \cdot D_2^2. \tag{5}$$

The right cross subarea S_{right} could be calculated based on the cost equilibrium conditions under the cost function to find the vertical line with the coordinate (x, y), as shown in Fig. 8, i.e.

$$c_1(q) + t \cdot r_1^2 = c_2(q) + t \cdot r_2^2. \tag{6}$$

Let $c_i(q) = A \cdot p_i(q)$ and $A = \xi \cdot t$, where A denote the storage cost index, ξ denote the ratio between A and t, then we have $\xi \cdot p_1(q) + (x^2 + y^2 + h_1^2) = \xi \cdot p_2(q) + ((D_{12} - x)^2 + y^2 + h_2^2)$. Therefore, we could get the coordinate of vertical line as

$$x = \frac{D_{12}}{2} + \frac{h_2^2 - h_1^2}{2D_{12}} + \frac{\xi \cdot [p_2(q) - p_1(q)]}{2D_{12}} \tag{7}$$

where, the first part of abovementioned formula denotes the central point of the line-of-circles, the second part denotes the altitude difference effect, and the third part denotes the storage cost difference effect. Therefore, we could get the right cross subarea S_{right} shown as

$$S_{\text{right}} = \beta \cdot D_1^2 - \sin\beta\cos\beta D_1^2 = \left(\beta - \frac{1}{2}\sin 2\beta\right) \cdot D_1^2 \tag{8}$$

where $\beta = \arccos\left(\frac{D_{12}^2 + h_2^2 - h_1^2 + \xi \cdot [p_2(q) - p_1(q)]}{2D_1 \cdot D_{12}}\right)$.

Then, we get the cross coverage area belonging to Orbiter 1 as $A_1 = S_{\text{cross}} - S_{\text{right}} = S_1 + S_2 - S_{\text{right}}$, and the cross coverage area belonging to Orbiter 2 as $A_2 = S_{\text{right}}$.

b) Utilize edge forwarding term d_{Ep12} to evaluate the dynamic changes of cross coverage area: The dynamic changes of cross coverage area in Mars relay missions could be classified into three stages, which is measured by the edge forwarding term d_{Ep12}, as described in the following.

Stage 1: No cross coverage area:

This stage is not considered due to no cross coverage area, as shown in Fig. 11, where $E_{p2} \geq E_{p1}$, $d_{Ep12} = E_{p1} - E_{p2} \leq 0$.

Stage 2: Cross coverage area at the left side of large circle:

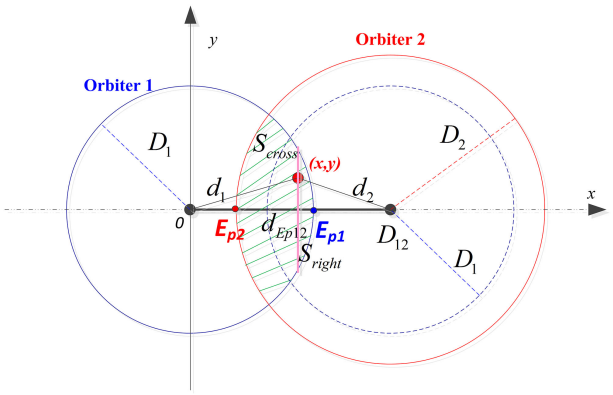

Fig. 12. Geometric model of stage 2.

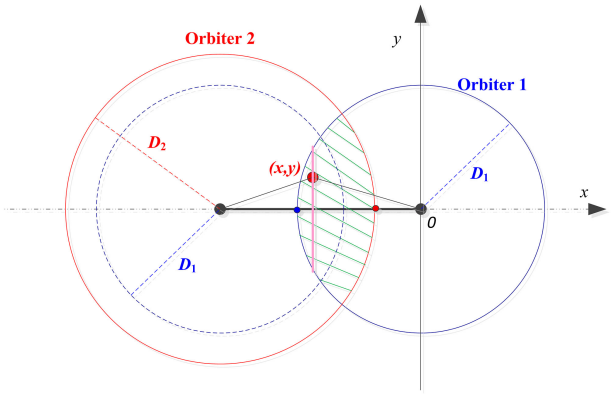

Fig. 13. Geometric model of stage 3.

Our research in this article mainly focuses on this stage, as shown in Fig. 12, where the parameters are defined as follows:

1) Lower Boundary: $E_{p2} < E_{p1}$, $d_{Ep12} = E_{p1} - E_{p2} > 0$.
2) Upper Boundary: $d_{Ep12} = E_{p1} - E_{p2} < D_1 + D_2$, shown as the dotted circle inside the large circle.

Stage 3: Cross coverage at right side of large circle:

This stage is the geometric mirror image of stage 2, as shown in Fig. 13, without further analysis.

c) Utilize relative geometric weight $w(d_{Ep12})$ to evaluate the rover's changing distribution probability: The relative geometry between two orbiters is measured by edge forwarding term d_{Ep12}, which denotes certain specific contact scenario including all of the possible angles from 0 to 2π between x axis and D_{12} vector, and the relative geometry weight of different contact scenarios in stage 2 could be calculated by the cumulative rings' area with increasing d_{Ep12} inside the big circle, which ranges from 0 to $D_1 + D_2$.

The relative geometric weight could be divided into three phases, as shown in Fig. 14, through the calculation we could get piecewise function of the relative geometric weight as follows:

$$w(d_{Ep12}) = \begin{cases} \gamma \cdot \pi \cdot [d_{Ep12}(2D_2 - d_{Ep12})], & \text{Phase 1} \\ \gamma \cdot \pi \cdot [D_2^2 + (d_{Ep12} - D_2)^2], & \text{Phase 2} \\ \gamma \cdot \pi \cdot [D_2^2 + (2D_1 - D_2)^2], & \text{Phase 3} \end{cases} \tag{9}$$

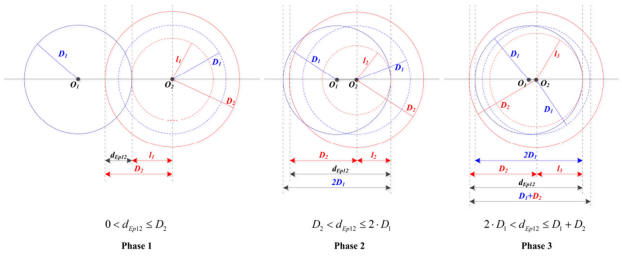

Fig. 14. Three phases of the relative geometric weight in stage 2.

where γ denotes the normalization weight index. The integral of piecewise (9) is shown as

$$\begin{aligned} w_{\text{total}} &= w_1 + w_2 + w_3 \\ &= \gamma \cdot \pi \cdot D_2^2 \left(-2D_1 + \frac{4}{3}D_2 + 4\frac{D_1^2}{D_2} - \frac{4}{3}\frac{D_1^3}{D_2^2} \right). \end{aligned} \tag{10}$$

Let the total weight $w_{\text{total}} = 1$, then we have the normalization weight index γ as

$$\gamma = \left\{ \pi \cdot D_2^2 \left(-2D_1 + \frac{4}{3}D_2 + 4\frac{D_1^2}{D_2} - \frac{4}{3}\frac{D_1^3}{D_2^2} \right) \right\}^{-1}. \tag{11}$$

Then, we could get the normalized relative geometry weight w as

$$w(d_{Ep12}) = \begin{cases} \dfrac{d_{Ep12}(2D_2 - d_{Ep12})}{D_2^2\left(-2D_1 + \frac{4}{3}D_2 + 4\frac{D_1^2}{D_2} - \frac{4}{3}\frac{D_1^3}{D_2^2} \right)}, & \text{Phase 1} \\ \dfrac{D_2^2 + (d_{Ep12} - D_2)^2}{D_2^2\left(-2D_1 + \frac{4}{3}D_2 + 4\frac{D_1^2}{D_2} - \frac{4}{3}\frac{D_1^3}{D_2^2} \right)}, & \text{Phase 2} \\ \dfrac{D_2^2 + (2D_1 - D_2)^2}{D_2^2\left(-2D_1 + \frac{4}{3}D_2 + 4\frac{D_1^2}{D_2} - \frac{4}{3}\frac{D_1^3}{D_2^2} \right)}, & \text{Phase 3}. \end{cases} \tag{12}$$

4) *NE Solution:* Given the two orbiters' storage status $q_1 = q_2 = q_f = 70\%$ as constant, we get the storage utility functions of the Orbiters 1 and 2 as

$$\begin{cases} u_1(p_1, p_2, d_{Ep12}) = p_1 \cdot A_1(p_1, p_2, d_{Ep12}) \cdot w(d_{Ep12}) \\ u_2(p_1, p_2, d_{Ep12}) = p_2 \cdot A_2(p_1, p_2, d_{Ep12}) \cdot w(d_{Ep12}). \end{cases} \tag{13}$$

Given the first order differential conditions as $\frac{\partial u_i}{\partial p_i} = 0$ $(i = 1, 2)$, we get the NE equation set with variables p_1, p_2 as

$$\begin{cases} S_1(d_{Ep12}) + S_2(d_{Ep12}) - S_{\text{right}}(p_1, p_2, d_{Ep12}) \\ \qquad - p_1 \cdot \frac{\partial S_{\text{right}}(p_1, p_2, d_{Ep12})}{\partial p_1} = 0 \\ S_{\text{right}}(p_1, p_2, d_{Ep12}) + p_2 \cdot \frac{\partial S_{\text{right}}(p_1, p_2, d_{Ep12})}{\partial p_2} = 0. \end{cases} \tag{14}$$

This is a typical nonlinear transcendental equation set, which could be solved by the iterative mathematic method. The solution of such nonlinear transcendental equation set is $\{p_1(d_{Ep12}), p_2(d_{Ep12})\}$ with variable d_{Ep12}. Then, we could further calculate the weighted price ratio $[c_i(q_f)/c_j(q_f)]$ as

$$\left[\frac{c_i(q_f)}{c_j(q_f)}\right] = \frac{\int \left[p_1(d_{Ep12})/p_2(d_{Ep12})\right] \cdot w(d_{Ep12}) \cdot d(d_{Ep12})}{\int w(d_{Ep12}) \cdot d(d_{Ep12})}. \tag{15}$$

C. Storage Cost

In this article, the storage cost function is designed as the power function $c(q) = A(1-q)^{-\alpha}$, where q denotes the percentage of utilized storage space, A denotes the storage cost index $(A > 0)$, α denotes the power factor. Next, we analyze the effective range of parameters and verify the results.

1) *First-Order Derivative:* The first-order derivative of function $c(q)$ is shown as

$$c'(q) = \alpha \cdot \left(1 - q\right)^{-\alpha - 1}. \tag{16}$$

The first-order derivative value of function $c(q)$ is mainly determined by parameter α: if $\alpha = 0$, then the orbiter would provide the data relay service with the same price in any situation, which ignores the effects of different storage status; if $\alpha < 0$, then the orbiter would provide the data relay service with lower price at higher storage percentage, which is contrary to the principle of scarcity of resources in economics. Therefore, the value of α should be larger than 0, that is $\alpha > 0$.

2) *Second-Order Derivative:* The second-order derivative of function $c(q)$ is shown as

$$c''(q) = \alpha \cdot (1 + \alpha) \cdot \left(1 - q\right)^{-\alpha - 2}. \tag{17}$$

If $\alpha > 0$, then $c''(q) > 0$. It means that if the orbiter is of the larger available storage space (the lower utilized storage percentage q), then the system would gain less marginal utility as lower storage cost on unit data volume. It coincides with the economic marginal utility theory, that is, the more quantity you could get from the market, the less utility you actually gain from the same commodity in unit. Under the deduction result of the first-order derivative as $\alpha > 0$, we could get the second-order derivative $c''(q) > 0$, which prove that the power function $c(q) = (1-q)^{-\alpha}$ with $\alpha > 0$ coincides with classical economic market principle, suitable to the orbiter selection issues in Mars automatic relay communications.

D. Orbiter Selection

In this article, the CCSDS Proximity-1 protocols is used as the baseline, in order to compare with the other two methods, that is, generally used distance dependence selection in Earth satellite constellation cases, and our new proposed transmission-and-storage cost integrated dependence selection.

1) *CCSDS Proximity-1 Protocols:* CCSDS Proximity-1 protocols could be described as "single access, first-in first-serve," which means that the rover only selects the first successfully hailed orbiter and communicates with this orbiter at each time slot until the end of current contact period.

2) *Distance Dependence Selection:* For the distance dependence selection algorithm, the rover selects the orbiter with minimum space distance at each time slot. The selection criteria in τth time slot is shown as

$$j_\tau = \arg\min_i \left\{ r_{i,\tau} \right\} \tag{18}$$

where $r_{i,\tau}$ is the space distance from rover to Orbiter i in τth time slot.

3) *Our Algorithm: Minimum Entire System Cost Selection:* For our algorithm, the rover selects the orbiter with minimum entire system cost at each time slot, including both the transmission cost and storage cost. Here, we utilize the equivalent parameter conversion to define the transmission cost and storage cost optimal selection rules, which means that the selected orbiter should satisfy such equivalent condition that transmission cost could be calculated by the space distance and the storage cost could evaluate the on-orbit energy consumption. The selection criteria in τth time slot for the minimum entire system cost method is shown as

$$j_\tau = \arg\min_i \left\{C_i(q_{i,\tau}, r_{i,\tau})\right\} \tag{19}$$

where

$$C_i(q_{i,\tau}, r_{i,\tau}) = \lambda \cdot c_i(q_{i,\tau}) + t(r_{i,\tau}) \tag{20}$$

$$c_i(q_{i,\tau}) = A \cdot (1 - q_{i,\tau})^{-\alpha_i} \tag{21}$$

$$q_{i,\tau} = \frac{V_{i,0} + V_{i,\tau}}{V_{\text{total}}} = \frac{V_{i,0} + \rho \cdot r_{i,\tau}^{-2}}{V_{\text{total}}} \tag{22}$$

V_{total} denotes the maximum buffer size, A denotes the power function efficient, $V_{i,0}$ denotes the Orbiter i's initial storage space, and $q_{i,\tau}$ denotes the storage percentage for orbiter i in τth time slot. Based on the data rates in Section II, the rover's access data rate is determined by the space distance $r_{i,\tau}$ between Rover and Orbiter i; therefore, the data volume $V_{i,\tau}$ sent from Rover to Orbiter i in τth time slot could be expressed as $V_{i,\tau} = \rho \cdot r_{i,\tau}^{-2}$, where ρ is used to convert the space distance to data volume, and $\lambda = 1$, which means that both the transmission cost and the storage cost have the equal weight of influence on the orbiter selection decision in this algorithm.

IV. SIMULATION RESULTS

A. Simulation Situation

In this article, the repeated ground track orbit is chosen as the orbit model, which was first defined and studied as Flower Constellation with the corresponding applications in telecommunication services in [19]–[21]. The repeating planet surface track design with N_p revolutions over N_d days (generally integers) is shown as

$$N_p \cdot T_O = N_d \cdot T_G \tag{23}$$

where T_O is the nodal period of the orbit, and T_G is the nodal period of Greenwich. Equation (23) could be further improved by the satellite orbit elements $[a, e, i, \Omega, \omega, M]$ in the central planet Mars as follows:

$$N_p \cdot \frac{2\pi}{\sqrt{\mu/a^3} + \omega' + M'} = N_d \cdot \frac{2\pi}{\omega_m - \Omega'} \tag{24}$$

where a is the semimajor axis, $\sqrt{\mu/a^3}$ is the orbit mean motion, e is the eccentricity, i is the inclination, Ω is the right ascension of ascending node (RAAN), ω is the argument of perigee, M is the mean anomaly, ω_m is the Mars rotation rate, Ω', ω', and M' are the time rate of the corresponding element's changes.

TABLE II
Repeated Ground Track Orbit Elements

Parameters	High altitude orbiter	Low altitude orbiter
Epoch time	1 Jan 2020 00:00:00.000 UTCG	
Repeated cycles/day	12	13
Altitude, h (km)	494.8808	292.7679
Eccentricity, e	0.0	0.0
Inclination, $i(^\circ)$	93.1	93.1
Argument of Perigee, $\omega(^\circ)$	80.0	310.0
RAAN, $\Omega_N(^\circ)$	140.118	95.118
Mean Anomaly, $M(^\circ)$	0.0	0.0

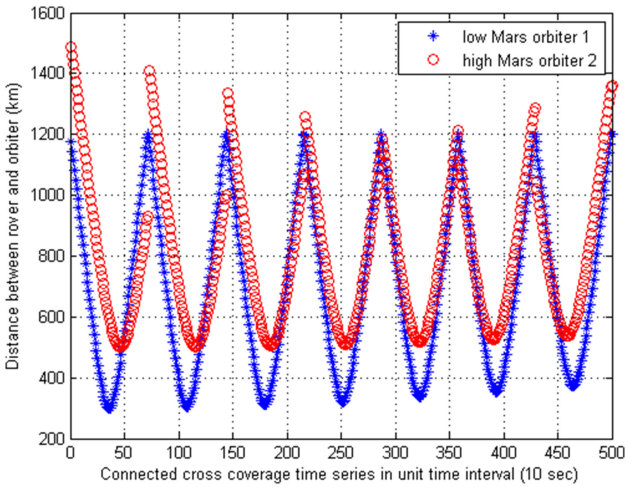

Fig. 15. Distance between the rover and orbiters with connected cross coverage time series.

In this simulation, the orbit parameters of two repeated ground track orbiters are shown in Table II, and the rover locates at the coordinate $(30^\circ N, 15^\circ E)$ on Mars surface. The space distance between the rover and orbiters with connected cross coverage time series in certain contact periods could be seen in Fig. 15. Through the analysis on the contact events, we find that the observation intersection of two orbiters in view of single rover is about 47.55% of the observation union, which proves that the observation intersection (cross coverage) is a common Mars relay communication scenario in this simulation situation, so that the orbiter selection optimization algorithms could play an important role and benefit entire system obviously. In addition, in our simulation the total available buffer size for data transmission is calculate by the upper bound of data transmitted by any single orbiter independently, which could be simplified by the equation $\text{datarate}_{\text{mean}} \times t_{\text{total}} = 2{,}048 \text{ kb/s} \times 10^4 \text{s} = 20.48 \text{ Gb} = 2.56 \text{ GB}$.

B. Improved Hotelling NE

The simulation results of the improved Hotelling NE could be seen as follows.

1) *NE Price:* The NE price solution is converted into unit price in Fig. 16, changing with the diverse edge forwarding terms. From the simulation result, we find that the NE price of low Mars orbiter is always larger than high Mars orbiter. In general, the low Mars orbiter requires more

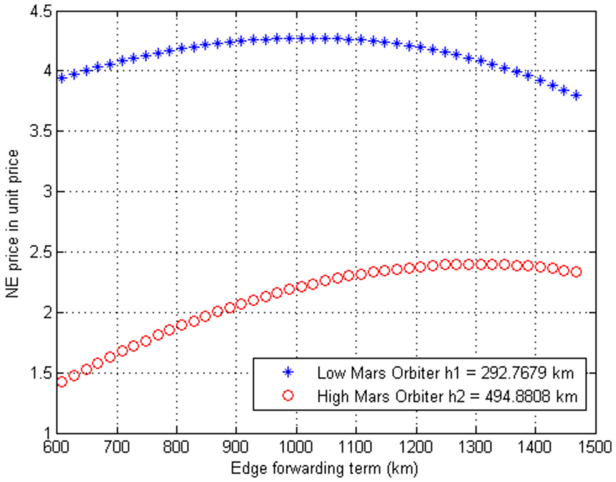

Fig. 16. NE price.

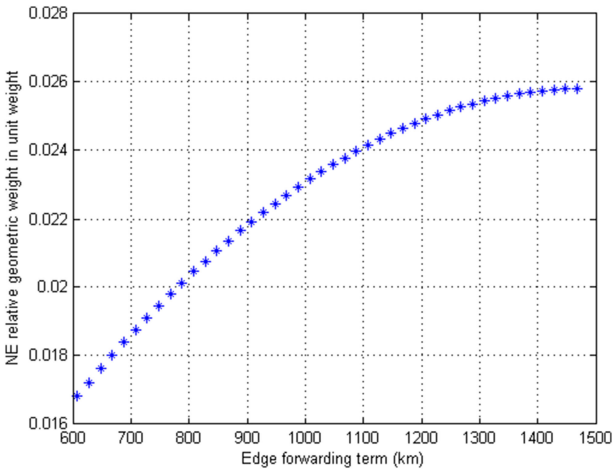

Fig. 17. NE relative geometric weight.

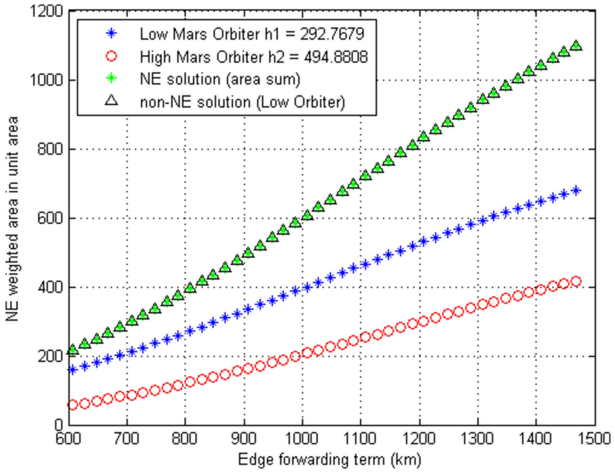

Fig. 18. NE weighted area.

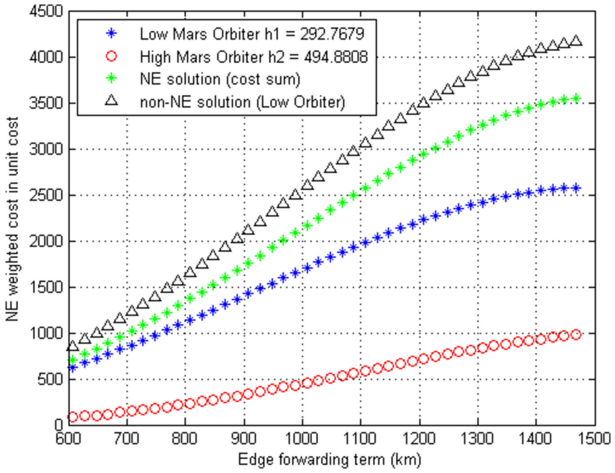

Fig. 19. NE weighted cost.

complex and frequent orbit adjustment operations with more fuel consumption due to the orbital perturbation and atmospheric drag. Meanwhile, there are usually more observation tasks assigned for the lower altitude orbiters, which requires necessary storage space reserved for such scientific goals. Therefore, the NE price solution is reasonable and coincides with the actual space engineering situation.

2) *NE Relative Geometric Weight:* The NE relative geometric weight is converted into unit weight shown in Fig. 17, changing with the diverse edge forwarding terms. The NE relative geometric weight increases with the edge forwarding term. Based on the simulation results from Figs. 16 and 17, the price ratio curve is calculated based on the different NE prices from two orbiters, and the weighted price ratio value is 1.9543 by the multiplication of price ratio with the NE relative geometric weight, which is the value of the storage cost ratio $c_1(q)/c_2(q)$ at $q_f = 0.7$. The reason why we choose the storage percentage 70% as the reference is that it reflects the conventional safety threshold for buffer usages, which could be managed by specific mission requirements.

3) *NE Weighted Area and Cost:* The corresponding NE weighted area and cost associated with the NE solutions are shown in Figs. 18 and 19, respectively, changing with the diverse edge forwarding terms. Simulation results show that, even if the independent coverage area of non-NE solution by low Mars orbiter is identical to the cross coverage area of NE solution by two orbiters as shown in Fig. 18, the weighted cost of non-NE solution is always larger than NE solution, which indicates that the NE solution of the improved Hotelling model could provide better cost saving data relay services.

C. Storage Cost Function

Based on the value of the storage cost ratio $c_1(q)/c_2(q)$ at $q_f = 0.7$ from previous procedures, we could get the storage cost curves of different orbiters with power index α_1, α_2, respectively. Assuming that the low attitude Orbiter 1's power index is $\alpha_1 = 1.0$, then, we have

$$c_1(q) = A \cdot (1-q)^{-\alpha_1}|_{q_f=0.7} = A \cdot (1-0.7)^{-1.0} \quad (25)$$

$$c_2(q) = A \cdot (1-q)^{-\alpha_2}|_{q_f=0.7} = A \cdot (1-0.7)^{-\alpha_2} \quad (26)$$

$$\frac{c_1(q_f)}{c_2(q_f)} = (1-0.7)^{\alpha_2-1} = 1.9543 \Rightarrow \alpha_2 = 0.44347. \quad (27)$$

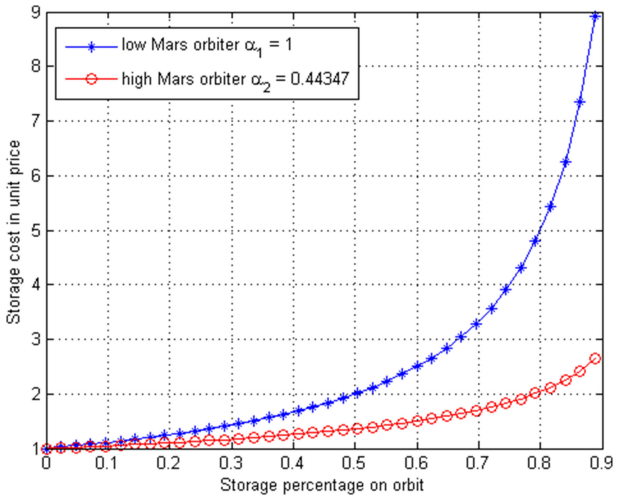

Fig. 20. Storage cost curve of different orbiters with diverse storage percentage.

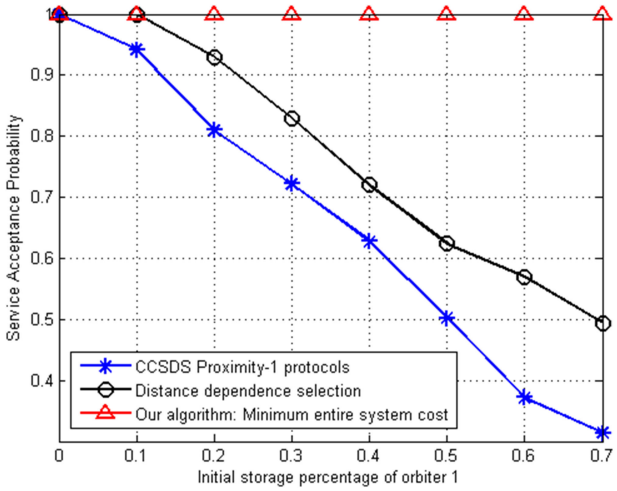

Fig. 21. Performance comparison of service acceptance probability.

The storage cost curve of different orbiters with increasing storage percentage is shown in Fig. 20.

D. Orbiter Selection

Three optimal selection algorithms described in Section III are modeled and compared with each other in the following simulation tests, with the statistical measurements as service acceptance probability, entire transmission volume, and system cost on unit transmission volume.

1) *Service Acceptance Probability:* Service acceptance probability (SAP) is the statistical mean value of the data relay services successfully accepted divided by the services arrived at the orbiters. The acceptance of certain data relay service is mainly decided on the remaining storage space of the selected orbiter, which means that if there were no adequate storage space to keep the data volumes in buffer in current time slot, the data relay service would be rejected and the data would be discarded. The performance comparison of different algorithms about the service acceptance fraction is shown in Fig. 21. The simulation results show the following.

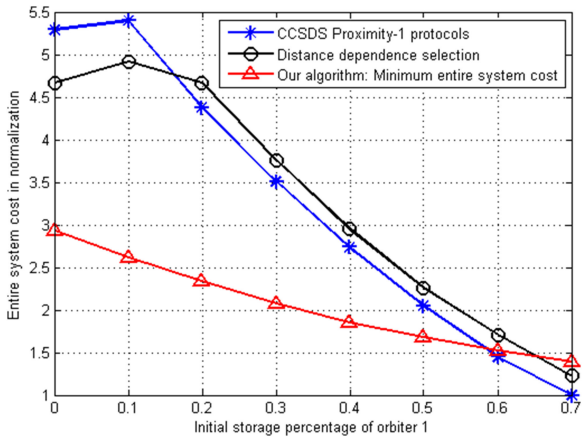

Fig. 22. Performance comparison of entire system cost.

1) The SAP values of both CCSDS Proximity-1 protocols and distance dependence selection algorithm decrease with the increasing initial storage percentage, which indicates that the service reject probability becomes larger when the orbiter has less storage space to store the data volume based on CCSDS Proximity-1 protocols and distance dependence selection algorithm.
2) The SAP value of distance dependence selection algorithm performs better than CCSDS Proximity-1 protocols, because CCSDS Proximity-1 protocols only selects the lower altitude Orbiter 1 with faster orbit phase velocity, which contributes to the earlier contact chance with the rover, but the storage buffer of lower altitude Orbiter 1 is also filled with data quickly.
3) The SAP value of our algorithm equals to 1.0, which indicates that our algorithm could provide the data relay service without any rejection.

2) *Entire System Cost:* In this simulation, we make the minimum value of all three algorithms as the reference 1.0, and calculate the ratio of the other algorithms by normalization, as shown in Fig. 22. The simulation results show the following.

1) For CCSDS Proximity-1 protocols, the rover only selects the lower altitude Orbiter 1 with higher system cost, but the rejection of services also contributes to the decrease of system cost; therefore, the curve is a little lower than distance dependence selection algorithm with the quicker descent of the service acceptance probability as shown in Fig. 21.
2) For distance dependence selection algorithm, it selects the orbiter only by the transmission cost, whose entire system cost is the highest in all three algorithms and quickly decreases by the increasing initial storage percentage. In this algorithm, the low altitude Orbiter 1 would be chosen as the access point in high probability due to the smaller space distance, even if Orbiter 1 has larger storage cost as shown in Fig. 20. The decrease of its system cost curve is due to the increase of service rejection as shown in Fig. 21.

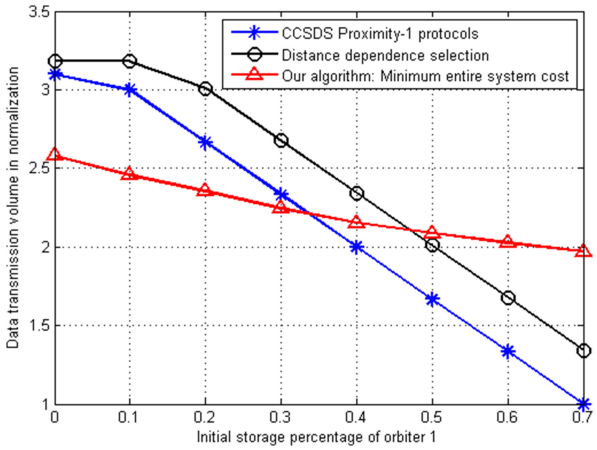

Fig. 23. Performance comparison of data transmission volume.

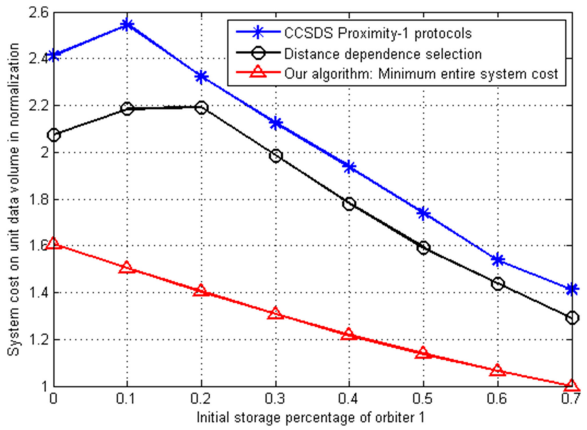

Fig. 24. Performance comparison of system cost on unit data volume.

3) For our algorithm, it selects the orbiter both by the transmission cost and the storage cost, whose entire system cost is the lowest in all three algorithms. In this algorithm, the higher altitude Orbiter 2 would be chosen as the access point in higher probability than the other two algorithms due to smaller storage cost in unit price as shown in Fig. 20.

3) *Data Transmission Volume:* In this simulation, we make the minimum value of all three algorithms as the reference 1.0, and calculate the ratio of the other algorithms by normalization, as shown in Fig. 23. The simulation results show the following.

1) For CCSDS Proximity-1 protocols, the rover only selects the lower altitude Orbiter 1 with smaller space distance for most time slots, but the rejection of services also contributes to the decrease of data transmission volume; therefore, the curve is lower than distance dependence selection algorithm with the decrease of the service acceptance probability as shown in Fig. 21.
2) For distance dependence selection algorithm, it selects the orbiter only by the transmission cost, whose performance quickly decreases by the increasing initial storage percentage of low altitude Orbiter 1. In this algorithm, the low altitude Orbiter 1 is chosen as the access point in high probability due to the smaller space distance. However, with the increasing percentage of the storage space in lower orbiter used for other exploration purpose, it would cause the entire system performance into degradation, because Orbiter 1 would refuse the data relay service as shown in Fig. 21.
3) For our algorithm, it selects the orbiter both by the transmission cost and the storage cost, whose performance is better than other two algorithms when the initial storage percentage is larger than 50%. Besides, the curve slowly decreases by the increasing initial storage percentage due to equalization effect from storage cost. In this algorithm, the higher altitude Orbiter 2 would be chosen as the access point in higher probability than the other two algorithms due to smaller storage cost in unit price as shown in Fig. 20, even if such orbiter transmits less data transmission volume by the larger space distance from the rover.

4) *System Cost on Unit Data Volume:* These curves in Fig. 24 are calculated by the division of the entire system cost and data transmission volume in each algorithm. The simulation results show the following.

1) For all algorithms, the entire system cost curve slop is larger than the data transmission volume curve slop, so that system cost on unit data volume decreases with increasing initial storage percentage.
2) The other two algorithms perform better than CCSDS Proximity-1 protocols with the enhancement as 9.31% and 36.14%, respectively, which proves that optimal orbiter selection really helps improving the system performance compared with current CCSDS Proximity-1 protocols.
3) For distance dependence selection algorithm, the entire system cost and data transmission volume are both larger than the other two algorithms. As shown in Figs. 22 and 23, the ratio of entire system cost between distance dependence selection algorithm and our algorithm is larger than the ratio of data transmission volume, therefore, the distance dependence selection algorithm has higher system cost on unit data volume than our algorithm.
4) Our algorithm has the lowest system cost on unit data volume and outperforms the distance dependence algorithm with the selection gains as 29.59% in statistical mean values.

The simulation results prove that the distance dependence selection and our algorithm both perform better than CCSDS Proximity-1 protocols with the balance of service acceptance fraction, transmission volume, entire system cost and its corresponding value on unit data volume, and our new algorithm "minimum entire system cost" selection algorithm performs best in all three algorithms, which is the most cost efficient in the multiple orbiter access for Mars relay communications.

V. CONCLUSION

This article studies the cost efficient orbiter selection algorithms in Mars relay communications based on the serial optimization architecture. The classical oligopoly Hotelling game is improved to adapt to the geometric characteristics of multiple orbiters in view of single rover, whose NE solutions could be used to determine the storage cost function of each orbiter. Meanwhile, the new minimum entire system cost selection algorithm performs better than other algorithms with the balance of service acceptance probability, data transmission volume, and entire system cost on unit data volume, which could be considered as the option for performance improvement in future Mars automatic relay communications.

Next, with the research on current Mars orbiter maneuver, we will study the cost and feasibility of our algorithm in deep space missions, including the computation complexity analysis and storage complexity analysis, and make necessary algorithm improvements to consider the storage cost as another variable besides transmission cost in the NE situation.

REFERENCES

[1] P. Wan, Y. Zhan, and X. Pan
Solar system interplanetary communication networks: Architectures, technologies and developments
Sci. China Inf. Sci., vol. 61, no. 4, 2018, Art. no. 040302.

[2] B. Du, F. Gao, and J. Xu
The analysis of topology based on Lagrange points L4/L5 of Sun-Earth system for relaying in Earth and Mars communication
In *Proc. IEEE 9th Int. Conf. Commun. Softw. Netw.*, 2017, pp. 533–537.

[3] P. Wan and Y. A. Zhan
Structured solar system satellite relay constellation network topology design for Earth-Mars deep space communications
Int. J. Satell. Commun. Netw., vol. 37, pp. 292–313, 2019.

[4] M. D. Sanctis, T. Rossi, M. Lucente, M. Ruggieri, D. Mortari, and D. Izzo
Flower constellation of orbiters for martian communication
In *Proc. IEEE Aerosp. Conf.*, Big Sky, MT, USA, 2007, pp. 1–11.

[5] M. D. Sanctis, T. Rossi, M. Lucente, M. Ruggirei, and D. Mortari
Space system architectures for Interplanetary Internet
In *Proc. IEEE Aerosp. Conf.*, Big Sky, MT, USA, 2010, pp. 1–8.

[6] D. Allard and R. Gladden
Mars relay operations service (MAROS): Managing strategic and tactical relay for the evolving Mars network
In *Proc. IEEE Aerosp. Conf.*, 2012, pp. 1–11.

[7] C. D. Edwards, D. J. Bell, and A. Biswas
Proximity link design and performance options for a Mars aerostationary relay satellite
In *Proc. Aerosp. Conf.*, 2016, pp. 1–10.

[8] CCSDS *PROXIMITY-1 Space Link Protocol-Rationale, Architecture, and Scenarios*, CCSDS, Washington, DC, USA, Tech. Rep. CCSDS 210.0-G-2, 2013.

[9] M. Andre, B. Andrea, and T. Ramona
DESCANSO Design and Performance Summary Series Article 6: Odyssey Telecommunications. Washington, DC, USA: NASA, 2002.

[10] J. Taylor, D. K. Lee, and S. Shambayati
DESCANSO Design and Performance Summary Series Article 12: Mars Reconnaissance Orbiter Telecommunications, Washington, DC, USA: NASA, 2006.

[11] M. Andre, I. Peter, and T. Jim
DESCANSO Design and Performance Summary Series Article 14: Mars Science Laboratory Telecommunications System Design, Washington, DC, USA: NASA, 2009.

[12] P. Wan, Y. Zhan, X. Pan, and L. Huang
Scheduling algorithm for the multiple rovers' access to single orbiter on the Mars relay communication links
Int. J. Satell. Commun. Netw., vol. 37, no. 6, pp. 612–629, Nov./Dec. 2019.

[13] H. Zhang, F. Sun, and F. Xu
Studies on access strategy of layered satellite networks
Comput. Eng. Des., vol. 26 no. 5, pp. 1121–1124, 2005.

[14] *Proximity-1 Space Link Protocol—Data Link Layer*, Issue 5. Recommended Standard (Blue Book), CCSDS 211.0-B-5, CCSDS, Washington, DC, USA, Dec. 2013.

[15] *Proximity-1 Space Link Protocol-Physical Layer*, Issue 4. Recommended Standard (Blue Book), CCSDS 211.1-B-4. CCSDS, Washington, DC, USA, Dec. 2013.

[16] *Proximity-1 Space Link Protocol-Coding and Synchronization Sublayer*, Issue 2. Recommended Standard (Blue Book), CCSDS 211.2-B-2, CCSDS, Washington, DC, USA, Dec. 2013.

[17] Y. Zhu
An analysis of influence of satellite design lifetime
Spacecraft Eng., vol. 16 no. 4, pp. 9–18, 2007.

[18] H. Hotelling
The stability in competition
Econ. J., vol. 39, pp. 41–57, 1929.

[19] D. Mortari and M. P. Wilkins
Flower constellation set theory. Part I: Compatibility and phasing
IEEE Trans. Aerosp. Electron. Syst., vol. 44, no. 3, pp. 953–962, Jul. 2008.

[20] M. P. Wilkins and D. Mortari
Flower constellation set theory part II: Secondary paths and equivalency
IEEE Trans. Aerosp. Electron. Syst., vol. 44, no. 3, pp. 964–976, Jul. 2008.

[21] D. Mortari, M. D. Sanctis, and M. Lucente
Design of flower constellations for telecommunication services
Proc. IEEE, vol. 99, no. 11, pp. 2008–2019, Nov. 2011.

Peng Wan (S'19) received the B.S. degree in physics from Peking University, Beijing, China, in 2004, and the M.S. degree in electronic engineering from Tsinghua University, Beijing, China, in 2007. He is currently working toward the Ph.D. degree in aeronautical and astronautical science and technology with the Space Center, Tsinghua University, Beijing, China.

His research interests include the system design of space TT&C network and deep space communications.

Yafeng Zhan received the B.S. and Ph.D. degrees in electronic engineering from the Department of Electronic Engineering, Tsinghua University, Beijing, China, in 1999 and 2004, respectively.

He is currently an Associate Professor with the Space Center, Tsinghua University. His current research interests include communication signal processing and deep space communications.

Xiaohan Pan received the B.Eng. degree in electronic engineering from the Dalian University of Technology, Dalian, China, in 2015. She is currently working toward the Ph.D. degree in information and communication engineering with the Space Center, Tsinghua University, Beijing, China.

Her research interests include the satellite constellation topology optimizations and satellite communications.